Trace mercury migration and human exposure in typical mercury-emission areas by compound-specific stable isotope analysis

Xinbin Feng, Leiming Zhang, Jeroen E. Sonke, David Point, Laurence Maurice, Runsheng Yin, Muhammad Ubaid Ali, Chuan Wang, Chongyang Qin, Ping Li, et al.

Environment International 174 (2023) 107891

Contents lists available at ScienceDirect

Environment International

journal homepage: www.elsevier.com/locate/envint

Full length article

Trace mercury migration and human exposure in typical mercury-emission areas by compound-specific stable isotope analysis

Bo Wang [a,b], Shaochen Yang [a], Ping Li [a,*], Chongyang Qin [a], Chuan Wang [a], Muhammad Ubaid Ali [a], Runsheng Yin [c], Laurence Maurice [d], David Point [d], Jeroen E. Sonke [d], Leiming Zhang [e], Xinbin Feng [a]

[a] State Key Laboratory of Environmental Geochemistry, Institute of Geochemistry, Chinese Academy of Sciences, Guiyang 550081, China
[b] Health Management Center, the Affiliated Hospital of Guizhou Medical University, Guiyang 550009, China
[c] State Key Laboratory of Ore Deposit Geochemistry, Institute of Geochemistry, Chinese Academy of Sciences, Guiyang 550081, China
[d] Observatory Midi-Pyrénées, Geosciences Environment Toulouse Laboratory, Research Institute for the Development (IRD), University of Toulouse and CNRS, 31400, Toulouse, France
[e] Air Quality Research Division, Science and Technology Branch, Environment and Climate Change Canada, Toronto M3H 5T4, Canada

ARTICLE INFO

Handling Editor: Adrian Covaci

Keywords:
Rice
Fish
Hair
Methylmercury
Compound-specific isotope analysis
Source appointment

ABSTRACT

Anthropogenic mercury (Hg) emissions have increased significantly since the Industrial Revolution, resulting in severe health impacts to humans. The consumptions of fish and rice were primary human methylmercury (MeHg) exposure pathways in Asia. However, the lifecycle from anthropogenic Hg emissions to human MeHg exposure is not fully understood. In this study, a recently developed approach, termed MeHg Compound-Specific Isotope Analysis (CSIA), was employed to track lifecycle of Hg in four typical Hg-emission areas. Distinct Δ^{199}Hg of MeHg and inorganic Hg (IHg) were observed among rice, fish and hair. The Δ^{199}Hg of MeHg averaged at 0.07 ± 0.15 ‰, 0.80 ± 0.55 ‰ and 0.43 ± 0.29 ‰ in rice, fish and hair, respectively, while those of IHg averaged at − 0.08 ± 0.24 ‰, 0.85 ± 0.43 ‰ and − 0.28 ± 0.68 ‰. In paddy ecosystem, Δ^{199}Hg of MeHg in rice showed slightly positive shifts (~0.2 ‰) from those of IHg, and comparable Δ^{199}Hg of IHg between rice grain and raw/processed materials (coal, Hg ore, gold ore and sphalerite) were observed. Simultaneously, it was proved that IHg in fish muscle was partially derived from *in vivo* demethylation of MeHg. By a binary model, we estimated the relative contributions of rice consumption to human MeHg exposure to be 84 ± 14 %, 58 ± 26 %, 52 ± 20 % and 34 ± 15 % on average in Hg mining area, gold mining area, zinc smelting area and coal-fired power plant area, respectively, and positive shifts of $\delta^{202}Hg_{MeHg}$ from fish/rice to human hair occurred during human metabolic processes. Therefore, the CSIA approach can be an effective tool for tracking Hg biogeochemical cycle and human exposure, from which new scientific knowledge can be generated to support Hg pollution control policies and to protect human health.

1. Introduction

Mercury (Hg) is a well-known toxic pollutant and global environmental and health concern. The organic form, methylmercury (MeHg), is extremely toxic to human's nervous, immune, and cognitive systems, causing nervous disorder, cardiovascular disease, and visual disturbance (Beckers et al., 2017; Clarkson et al., 2006; Selin, 2009). Anthropogenic activities have led to an elevation of Hg content in atmosphere, ocean, and terrestrial systems by a factor of 3 to 5 compared to the preindustrial period (Beckers et al., 2017; Driscoll et al., 2013; Selin, 2009), posing potential adverse impacts on humans and wildlife. In China, large amounts of Hg have been released to the environment via anthropogenic activities, and the main industrial sectors contributing to Hg emissions include coal combustion, cement production, zinc smelting, gold production and Hg mining (Wu et al., 2016). Anthropogenic Hg emissions to the atmosphere were estimated to be 444 tons in 2017 in China, which accounted for 17.6 % of total global anthropogenic emissions (Liu et al., 2019; UNEP, 2019). The released Hg can be transported into agricultural and aquatic ecosystems (Beckers et al., 2017; Zhang et al., 2021), where inorganic Hg (IHg) can be easily transformed into MeHg by

* Corresponding author.
E-mail address: liping@mail.gyig.ac.cn (P. Li).

https://doi.org/10.1016/j.envint.2023.107891
Received 31 December 2022; Received in revised form 17 February 2023; Accepted 16 March 2023
Available online 20 March 2023

microorganisms and subsequently bioaccumulated in the food webs. Previous studies reported that the MeHg concentrations in certain types of fish exceeded the national limit (carnivorous: 1000 ng/g; non-carnivorous: 500 ng/g) (Cheng et al., 2009; GB2762, 2017; Liu et al., 2014; Qiu et al., 2009; Shao et al., 2013). Rice can also bioaccumulate MeHg with the bioaccumulation factor being 800 times higher than that for IHg (Feng et al., 2008; Zhang et al., 2010b). Fish and rice consumption are considered as two primary pathways for human MeHg exposure in China (Cheng et al., 2009; Li et al., 2012; Liu et al., 2018; Zhang et al., 2010a). Comprehensive models have been developed for linking anthropogenic Hg emissions to human exposure at national and global scales (Chen et al., 2019; Zhang et al., 2021). However, limited tools are available to trace the migration and transformation behavior of Hg during the biogeochemical cycle, especially in typical Hg-emission areas.

Mercury isotopes are useful tracers for tracing Hg sources, translocation, and transformation processes of Hg in paddy fields and aquatic ecosystems (Kwon et al., 2020; Li et al., 2016; Li et al., 2017; Qin et al., 2020; Tsui et al., 2020; Yin et al., 2013a). Mass-dependent fractionation (MDF) arises in various physical, chemical, and biological processes, while mass-independent fractionation (MIF) is primarily induced by photoreduction of Hg(II) and photodegradation of MeHg (Blum et al., 2014; Kwon et al., 2020; Tsui et al., 2020). No significant MIF has been observed after absorption of Hg from the environment into rice plant and food webs (Kwon et al., 2014; Qin et al., 2020). Total Hg (THg) isotopes have been used to identify human Hg exposure sources and metabolic processes (Du et al., 2018; Laffont et al., 2009; Laffont et al., 2011; Li et al., 2014; Rothenberg et al., 2017; Sherman et al., 2013). For example, a significant MDF of ~ 2 ‰ for δ^{202}Hg and no MIF in THg between human hair and fish diet have been reported (Laffont et al., 2009; Laffont et al., 2011). The shift of δ^{202}Hg (~2‰) in THg was attributed to the assimilation of residual MeHg after demethylation, leading to accumulation of heavier Hg isotopes in hair and lighter Hg isotopes in urine (Du et al., 2020; Sherman et al., 2013). As rice and fish showed significantly different THg isotopic values, a binary mixing model based on Δ^{199}Hg has been used to quantify human exposure pathways (Du et al., 2018; Rothenberg et al., 2017). Recently, the online and offline determinations of the isotopic composition of different Hg species were conducted in natural samples, which found that MeHg and IHg in the biological materials were isotopically distinguishable (Epov et al., 2008; Li et al., 2017; Masbou et al., 2013; Perrot et al., 2016; Qin et al., 2020). MeHg and IHg isotopic composition in paddy ecosystem indicated that rice MeHg was derived from soil MeHg, and the Hg isotopes in aquatic ecosystem also can be used as a proxy for migration and transformation of MeHg (Li et al., 2017; Perrot et al., 2016; Qin et al., 2018; Qin et al., 2020). However, few studies used compound specific isotope analysis (CSIA) to assess human Hg exposure and Hg biogeochemical cycle in typical Hg-emission areas. Using CSIA may identify human exposure pathways of MeHg and better understand the environmental fate of Hg.

This study aims to quantify pathways of human MeHg exposure and identify migration processes of MeHg and IHg in typical Hg-emission areas. (Masbou et al., 2013; Yang et al., 2021) Isotopic compositions of MeHg and IHg in rice and fish samples were measured using a MeHg-CSIA approach, and then used to identify the migration processes of MeHg and IHg in the paddy field and aquatic ecosystems. The isotopic data of MeHg in hair samples were used to trace sources of human MeHg exposure.

2. Materials and methods

2.1. Study areas and sample preparation

Four typical Hg-emission areas in China were selected for investigation in this study, with the first three in Guizhou province and the fourth one in Hunan province (Fig. 1). The first area is adjacent to the largest coal-fired power plant (CFPPA) in the province, the second one is located in a large-scale gold mining area (GMA), the third one is located in a mercury mining area (MMA), and the fourth one is located in a zinc smelting area (ZSA) which is among the largest ones in China. The rice, fish muscle and human hair samples were collected and pretreated in the four areas in our previous study (Wang et al., 2021). Sample collection and preparation methods are described in detail in SI Section S1. In this study, the THg and MeHg concentrations are expressed as wet weight for fish muscle and dry weight for hair and rice samples. A total of 20 fish muscle, 21 rice and 21 hair samples were selected for Hg isotopic analysis in this study and THg and speciation analysis were presented in a previous study (Wang et al., 2021). The strategies for selecting samples are as follows: 1) main species of commonly consumed fishes being covered, which are listed in SI Table S1; 2) rice samples cultivated in local paddy fields; 3) no occupational exposure, dental amalgams and dyed hair for participants; and 4) paired hair and rice samples.

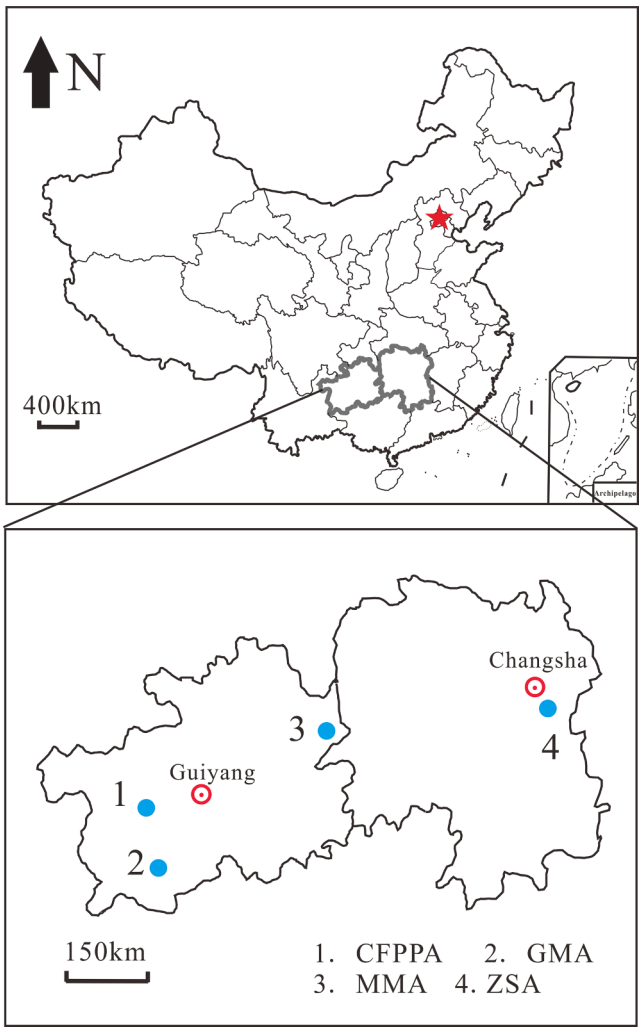

Fig. 1. Locations of the four study areas.

2.2. Total mercury and methylmercury analysis

To determine the concentrations of THg in fish, rice and human hair, the samples were acid digested and analyzed using cold vapor atomic fluorescence spectroscopy (CVAFS) (Du et al., 2018). For MeHg analysis, fish muscle, rice and hair samples were digested by 25 % w/w KOH, KOH/ methanol and 25 % v/v HNO_3, respectively (Du et al., 2018; Hintelmann et al., 2005; USEPA, 2002). Subsequently, the digested solutions were ethylated, purged, trapped and analyzed using GC-CVAFS

(using a MERX instrument, Brooks Rand instruments) consistently (Liang et al., 1996). Additionally, a selective extraction method (SEM) adopted from Yang et al. (2021) was used for MeHg isotope preparation. THg and MeHg concentrations of the extracted solutions were measured as described above. TORT-2 (Lobster hepatopancreas, National Research Council Canada) and ERM-CE464 (Tuna fish, European Reference Materials) were prepared with the same procedures to certify the effectiveness and precision of the SEM. Recovery and purity of MeHg were used to determine the extraction efficiency, ensuring that MeHg in samples was totally transferred into extracts and no IHg was incorporated (Table S2). The recoveries of MeHg in certified reference materials (CRMs), rice, fish muscle and hair samples showed an average of 93 ± 8 %, while the purities of MeHg in digested solutions averaged at 94 ± 7 %.

Method blanks, matrix spikes, CRMs and blind duplicates were measured to ensure quality control. Limit of determination (LOD) of THg was 0.03 ng/g for rice samples and 0.07 ng/g for human hair and fish samples. LOD of MeHg was 0.004 ng/g for all samples. The percentage of recoveries on spiked samples averaged 93 ± 8 % for MeHg in rice. In duplicate samples, the relative percentage differences were lower than 10 % for THg and MeHg. The average recoveries of THg and MeHg in CRMs were higher than 90 % (Table S2).

2.3. Hg isotope analysis

The digested and extracted solutions were analyzed for Hg isotopic composition using a Neptune Plus multi-collector inductively coupled plasma mass spectrometry at the State Key Laboratory of Environmental Geochemistry, Institute of Geochemistry, Chinese Academy of Science, following a method reported previously (Qin et al., 2020). δ^{202}Hg, Δ^{199}Hg, Δ^{200}Hg and Δ^{201}Hg were calculated following the protocol recommended by Bergquist et al. (2007) as follow:

$$\delta^{xxx_{Hg}}(\%) = \left[\left(xxx_{Hg}/198_{Hg_{sample}}\right)\Big/\left(xxx_{Hg}/198_{Hg_{NIST3133}}\right)\right]-1] \times 1000 \quad (1)$$

$$\Delta^{199}Hg = \delta^{199}Hg - \delta^{202}Hg \times 0.252 \quad (2)$$

$$\Delta^{200}Hg = \delta^{200}Hg - \delta^{202}Hg \times 0.502 \quad (3)$$

$$\Delta^{201}Hg = \delta^{201}Hg - \delta^{202}Hg \times 0.752 \quad (4)$$

where xxx is 199, 200, 201 or 202. NIST 3133 is adopted as a Hg isotope reference standard (Blum et al., 2007).

UM-Almadén standard solution was measured in every-eight samples to ensure the quality of the measurement. Lichen (BCR-482), fish (ERM-CE464) and hair (NIES-13) CRMs were measured to ensure no isotopic fractionation during the digested procedure. THg isotopic composition of UM-Almadén (δ^{202}Hg = − 0.56 ± 0.08 ‰, Δ^{199}Hg = − 0.01 ± 0.03 ‰, Δ^{200}Hg = − 0.01 ± 0.10 ‰, Δ^{201}Hg = − 0.01 ± 0.06 ‰, ±2σ, n = 16), BCR-482 (δ^{202}Hg = − 1.51 ± 0.12 ‰, Δ^{199}Hg = − 0.62 ± 0.08 ‰, Δ^{200}Hg = 0.07 ± 0.08 ‰, Δ^{201}Hg = − 0.65 ± 0.10 ‰, ±2σ, n = 4), ERM-CE464 (δ^{202}Hg = 0.83 ± 0.12 ‰, Δ^{199}Hg = 2.16 ± 0.08 ‰, Δ^{200}Hg = 0.09 ± 0.08 ‰, Δ^{201}Hg = 1.93 ± 0.10 ‰, ±2σ, n = 4) and NIES-13 (δ^{202}Hg = 1.84 ± 0.12 ‰, Δ^{199}Hg = 1.75 ± 0.08 ‰, Δ^{200}Hg = 0.06 ± 0.06 ‰, Δ^{201}Hg = 1.44 ± 0.08 ‰, ±2σ, n = 4) agreed well with previously reported results (Blum et al., 2014; Estrade et al., 2010; Masbou et al., 2013; Yamakawa et al., 2016).

The recoveries of MeHg in CRMs, rice, fish and hair samples showed an average of 93 ± 8 %, while the purities of MeHg in digested solutions averaged at 94 ± 7 %. MeHg isotopic compositions of TORT-2 (δ^{202}Hg = 0.45 ± 0.12 ‰, Δ^{199}Hg = 1.00 ± 0.08 ‰, Δ^{200}Hg = 0.16 ± 0.12 ‰, Δ^{201}Hg = 0.80 ± 0.08 ‰, ±2σ, n = 3) and ERM-CE464 (δ^{202}Hg = 0.72 ± 0.12 ‰, Δ^{199}Hg = 2.26 ± 0.08 ‰, Δ^{200}Hg = 0.11 ± 0.09 ‰, Δ^{201}Hg = 1.74 ± 0.08 ‰, ±2σ, n = 4) agreed well with previously reported results (Masbou et al., 2013).

Based on the isotopic values of THg and MeHg, the IHg isotopic values in rice, fish and hair samples were estimated by a binary mixing model as follows:

$$\delta^{202}Hg_{IHgi} = (\delta^{202}Hg_{THgi} - f_{MeHgi} \times \delta^{202}Hg_{MeHgi})/f_{IHgi} \quad (5)$$

$$\Delta^{199}Hg_{IHgi} = (\Delta^{199}Hg_{THgi} - f_{MeHgi} \times \Delta^{199}Hg_{MeHgi})/f_{IHgi} \quad (6)$$

$$\Delta^{200}Hg_{IHgi} = (\Delta^{200}Hg_{THgi} - f_{MeHgi} \times \Delta^{200}Hg_{MeHgi})/f_{IHgi} \quad (7)$$

$$\Delta^{201}Hg_{IHgi} = (\Delta^{201}Hg_{THgi} - f_{MeHgi} \times \Delta^{201}Hg_{MeHgi})/f_{IHgi} \quad (8)$$

$$f_{MeHgi} + f_{IHgi} = 1 \quad (9)$$

where f_{IHgi} and f_{MeHgi} are the IHg and MeHg fraction in sample i, respectively. A Monte Carlo simulation approach (n = 100,000 times), based on pseudorandom number generation function in RStudio Desktop (Open access for Windows), was utilized to calculate IHg isotopes. The standard deviation of f_{MeHgi} was lower than 5 % as computed by multiple measurements of the same samples. Two folds standard deviation of δ^{202}Hg, Δ^{199}Hg, Δ^{200}Hg and Δ^{201}Hg of UM-Almadén, which were 0.08, 0.06, 0.09 and 0.12 ‰, respectively, were adopted for assessing the uncertainties of THg and MeHg isotopic values. Even-MIF values were discussed in SI Section S2.

2.4. Human MeHg exposure from fish and rice consumption

In China, rice and fish are the main sources to human MeHg exposure (Li et al., 2012; Liu et al., 2018; Zhang et al., 2010a). Because there is no significant MIF occurring during metabolic and trophic transfer processes (Du et al., 2018; Laffont et al., 2009; Liu et al., 2018; Zhang et al., 2010a), MIF values in hair MeHg represent a mixture of those from fish and rice. A binary mixing isotope model, described in the following equations, can then be used to quantify the relative contribution of human MeHg exposure from fish and rice consumption:

$$\Delta^{199}Hg_{hairMeHgj} = f_{fishMeHgj} * \Delta^{199}Hg_{fishMeHgj} + f_{riceMeHgj} * \Delta^{199}Hg_{riceMeHgj} \quad (10)$$

$$f_{fishMeHgj} + f_{riceMeHgj} = 1 \quad (11)$$

where $\Delta^{199}Hg_{hairMeHgj}$, $\Delta^{199}Hg_{fishMeHgj}$ and $\Delta^{199}Hg_{riceMeHgj}$ are Δ^{199}Hg values of hair, fish and rice MeHg in area j, respectively; and $f_{fishMeHgj}$ and $f_{riceMeHgj}$ are relative MeHg contribution of fish and rice for human MeHg exposure, respectively. Area j represents MMA, GMA, CFPPA and ZSA, respectively. A Monte Carlo simulation approach (n = 100,000 times) was also used for calculating the contribution in RStudio Desktop (Open access for Windows).

2.5. Shifts of MDF of MeHg from diet to hair

To avoid the interference of $\delta^{202}Hg_{IHg}$, MDF of MeHg from dietary sources to hair samples could be used directly for identifying human MeHg exposure pathway in this study. As rice and fish consumption were the main pathways of human MeHg exposure, MDF of MeHg during human metabolic process was calculated using the following formula:

$$Shift_j = \delta^{202}Hg_{hairMeHgj} - f_{riceMeHgj} * \delta^{202}Hg_{riceMeHgj} - f_{fishMeHgj} * \delta^{202}Hg_{fishMeHgj}$$

Where $Shift_j$ is MDF value of MeHg from rice/fish to hair; and $\delta^{202}Hg_{hairMeHgj}$, $\delta^{202}Hg_{riceMeHgj}$ and $\delta^{202}Hg_{fishMeHgj}$ represent hair, rice and fish $\delta^{202}Hg_{MeHg}$ in study area j, respectively. $f_{fishMeHgj}$ and $f_{riceMeHgj}$ were calculated as mentioned above.

3. Results and discussion

3.1. Rice Hg and source appointment

The mean concentration of THg in rice in GMA (7.29 ± 1.85 ng/g),

CFPPA (7.93 ± 3.23 ng/g) and ZSA (8.47 ± 3.26 ng/g) showed comparable levels (Table 1). In comparison, rice THg concentrations in MMA (28.7 ± 24.1 ng/g) were significantly higher ($p < 0.05$). Similarly, rice MeHg concentrations in MMA (7.49 ± 2.55 ng/g) were also significantly higher than those in GMA (2.74 ± 2.83 ng/g), CFPPA (3.31 ± 1.66 ng/g), ZSA (4.84 ± 2.54 ng/g) and national background (1.37 ± 1.18 ng/g) (Xu et al., 2019; Zhao et al., 2019). The rice samples from the four areas were characterized by negative $\delta^{202}Hg_{THg}$ ($\delta^{202}Hg$ in THg) and near-zero $\Delta^{199}Hg_{THg}$ ($\Delta^{199}Hg$ in THg) (Fig. 2, Table S4). The $\delta^{202}Hg_{THg}$ in rice samples showed similar values among the four areas, with averages of − 2.07 ± 0.55 ‰ in MMA, −2.13 ± 0.74 ‰ in GMA, −2.01 ± 1.07 ‰ in CFPPA and − 1.81 ± 0.79 ‰ in ZSA. The average $\Delta^{199}Hg_{THg}$ values in rice samples were 0.03 ± 0.06 ‰, 0.07 ± 0.03 ‰, 0.06 ± 0.04 ‰ and − 0.01 ± 0.07 ‰ in MMA, GMA, ZSA and CFPPA, respectively.

Rice samples from the study areas showed negative $\delta^{202}Hg_{MeHg}$ ($\delta^{202}Hg$ in MeHg) values, with average values of − 0.78 ± 0.38 ‰ in MMA, −1.04 ± 0.26 ‰ in GMA, −1.19 ± 0.27 ‰ in CFPPA and − 0.91 ± 0.48 ‰ in ZSA (Fig. 2, Table S4). The average $\Delta^{199}Hg_{MeHg}$ ($\Delta^{199}Hg$ in MeHg) value in rice samples in ZSA (0.22 ± 0.07 ‰) was significantly higher ($p < 0.05$) than those in MMA (0.09 ± 0.07 ‰) and GMA (0.11 ± 0.08 ‰), while that in CFPPA showed a slightly negative value (−0.10 ± 0.12 ‰), indicating that MeHg in rice samples may be originated from different sources. A significant relationship ($r^2 = 0.89$, $p < 0.05$) was found between rice $\Delta^{199}Hg_{MeHg}$ and soil $\Delta^{199}Hg_{THg}$, suggesting that MeHg in rice grain was potentially derived from soil. Significant positive MIF was found from soil IHg to rice MeHg (e.g. soil MeHg) in the four study areas, with an average of 0.12 ± 0.05 ‰ in MMA, 0.24 ± 0.05 ‰ in GMA, 0.18 ± 0.09 ‰ in CFPPA and 0.25 ± 0.08 ‰ in ZSA. The total shifts of $\Delta^{199}Hg$ from IHg to MeHg averaged at ~ 0.2 ‰ in paddy soil. No MIF would occur during biotic methylation and demethylation processes, and only aqueous photodegradation for MeHg could cause significant MIF (Bergquist et al., 2007; Blum et al., 2014), suggesting the existence of aqueous MeHg photodegradation in the paddy field. Rice plants obstructed the primary sunlight in the paddy field, resulting in weak photochemical reaction and small MIF in the paddy ecosystem. These results suggest that MeHg isotopes could identify the sources of rice MeHg in different typical Hg-emission areas.

Average $\Delta^{199}Hg_{IHg}$ ($\Delta^{199}Hg$ in IHg) values of rice samples in MMA (−0.01 ± 0.12 ‰), GMA (0.03 ± 0.07 ‰) and CFPPA (0.06 ± 0.11 ‰) were close to zero, which were comparable to those of Hg ores (0.01 ± 0.02 ‰), gold ores (−0.03 ± 0.07 ‰) and coal (0.11 ± 0.09 ‰) (Sun et al., 2014; Yin et al., 2019; Yin et al., 2013b), respectively (Fig. 3). The rice $\Delta^{199}Hg_{IHg}$ values in ZSA (−0.14 ± 0.06 ‰) were slightly negative, which were similar to those in sphalerites (−0.16 ± 0.09 ‰) (Liu et al., 2021). Hence, $\Delta^{199}Hg_{IHg}$ values of rice samples can be used to trace the sources of IHg in the rice. Our previous study found that $\Delta^{199}Hg_{IHg}$ of rice grain showed same signal with that of air (Qin et al., 2020). We concluded that $\Delta^{199}Hg_{IHg}$ values of air in the study areas showed the same signals as those of used ore, coal and other raw materials. Therefore, total gaseous Hg concentrations and Hg isotopes of air were significantly impacted by these emission sources. The $\delta^{202}Hg_{IHg}$ ($\delta^{202}Hg$ in IHg) in rice samples showed notable negative values, with average values of − 3.23 ± 1.04 ‰ in MMA, −3.01 ± 1.59 ‰ in GMA, −2.83 ± 2.33 ‰ in CFPPA and − 2.70 ± 2.05 ‰ in ZSA. The $\delta^{202}Hg_{IHg}$ in rice samples showed lower values than those in raw ore materials and coal in the four study areas, with average shifts of − 2.49 ± 0.61 ‰ in MMA, −2.30 ± 1.07 ‰ in GMA, −1.10 ± 1.41 ‰ in CFPPA and − 3.76 ± 1.46 ‰ in ZSA (Fig. 3). The shifts could be explained by the following factors. During ore roasting and coal combustion processes, lighter Hg isotopes were easily emitted into atmosphere, with the shifts of $\delta^{202}Hg$ of − 1.1 ‰ to − 0.1 ‰ (Sun et al., 2014; Yin et al., 2013b). Additionally, lighter Hg isotopes were preferentially absorbed by foliage with a $\delta^{202}Hg$ shift of − 3.0 ‰ to − 1.0 ‰ from atmospheric input of Hg to foliage (Blum et al., 2014; Demers et al., 2013; Yuan et al., 2019), resulting in lower $\delta^{202}Hg_{IHg}$ values in rice samples than those of the emission sources. Therefore, $\Delta^{199}Hg_{IHg}$ and $\delta^{202}Hg_{IHg}$ in rice both provided valuable information on the pollution sources of Hg.

Table 1
THg and MeHg concentrations in rice, fish, and hair samples in four study areas. MMA: Hg mining area; GMA: gold-mining area; CFPPA: coal-fired power plant; ZSA: zinc smelter area.

Study area	Matrix	THg (ng/g)		MeHg (ng/g)		MeHg/THg (%)
		n	Mean ± SD	n	Mean ± SD	
MMA	Rice	5	28.7 ± 24.1	5	7.49 ± 2.55	39.3 ± 21.5
	Fish	4	12.4 ± 8.26	4	5.32 ± 2.85	45.2 ± 7.9
	Hair	5	2080 ± 1160	5	854 ± 368	44.3 ± 8.6
GMA	Rice	5	7.29 ± 1.85	5	3.06 ± 0.98	43.8 ± 14.6
	Fish	6	7.04 ± 6.69	6	2.74 ± 2.83	36.4 ± 9.7
	Hair	5	524 ± 481	5	313 ± 341	54.7 ± 11.1
CFPPA	Rice	5	7.93 ± 3.23	5	3.58 ± 0.98	47.2 ± 8.5
	Fish	5	6.80 ± 3.29	5	3.31 ± 1.66	49.4 ± 10.7
	Hair	5	220 ± 49.4	5	145 ± 47.5	65.3 ± 11.1
ZSA	Rice	6	8.47 ± 3.26	6	4.84 ± 2.54	56.0 ± 12.0
	Fish	5	13.9 ± 11.5	5	6.17 ± 4.30	50.3 ± 11.4
	Hair	6	637 ± 226	6	466 ± 208	71.3 ± 7.1

3.2. Fish Hg and source appointment

The mean concentrations of THg in fish were comparable between GMA (7.04 ± 6.69 ng/g) and CFPPA (6.80 ± 3.29 ng/g), and between MMA (12.4 ± 8.26 ng/g) and ZSA (13.9 ± 11.5 ng/g); however, the values were significantly higher ($p < 0.05$) in the latter than the former two areas. A similar trend was also observed for the mean concentrations of MeHg in fish, with average MeHg ratio to THg of 44.9 ± 11.1 % (range: 21 % to 69 %) in the four areas, which were comparable with the results found in the Three Gorges Dam and a Hg-contaminated reservoir (Liu et al., 2012; Xu et al., 2018). Such low MeHg ratio found in fish muscle was potentially attributed to short aquatic food chain and short growth time in aquaculture fish (Wang et al., 2019). The $\delta^{202}Hg_{THg}$ and $\Delta^{199}Hg_{THg}$ values in individual fish samples ranged from − 2.02 ‰ to 0.75 ‰ and from 0.05 ‰ to 2.02 ‰, respectively (Fig. 2, Table S4), which were comparable to those of fish collected from Guiyang, Wuhan, Zhoushan and Xiamen in China ($\delta^{202}Hg_{THg}$: −2.13 ‰~1.21 ‰; $\Delta^{199}Hg_{THg}$: 0.07 ‰~2.08 ‰) (Du et al., 2018; Meng et al., 2020; Yang et al., 2021).

The $\delta^{202}Hg_{MeHg}$ values in fish samples averaged at − 0.21 ± 0.41 ‰ in MMA, −0.08 ± 0.31 ‰ in GMA, −0.12 ± 0.62 ‰ in ZSA and 0.02 ± 0.25 ‰ in CFPPA (Fig. 2), while the $\Delta^{199}Hg_{MeHg}$ values in fish averaged at 0.50 ± 0.33 ‰ in MMA, 0.70 ± 0.55 ‰ in GMA, 1.04 ± 0.84 ‰in ZSA and 0.93 ± 0.22 ‰ in CFPPA. No significant differences in fish $\delta^{202}Hg_{MeHg}$ (or $\Delta^{199}Hg_{MeHg}$) were found among the four areas. The $\Delta^{199}Hg/\Delta^{201}Hg$ ratio in fish MeHg was 1.21 ± 0.06 (Fig. S2a), which was similar to those in THg of marine and freshwater fish (Bergquist et al., 2007; Blum et al., 2014; Du et al., 2018; Kwon et al., 2012). Therefore, before entering into fish body, MeHg in water undergo significant photodegradation and the residues inherit positive MIF signal (Blum et al., 2014; Tsui et al., 2020). Since $\Delta^{199}Hg_{MeHg}$ values in the sediment were close to zero (Janssen et al., 2015; Rosera et al., 2020), fish MeHg was likely mainly derived from euphotic zone, where visible light can induce MIF of Hg in water or a marine microalga, instead of sediment (Kritee et al., 2018; Yang et al., 2022). A previous study found that $\Delta^{199}Hg_{MeHg}$ of plankton samples from Lake Menota showed significantly positive values (1.62 ± 0.13 ‰) (Rosera et al., 2020),

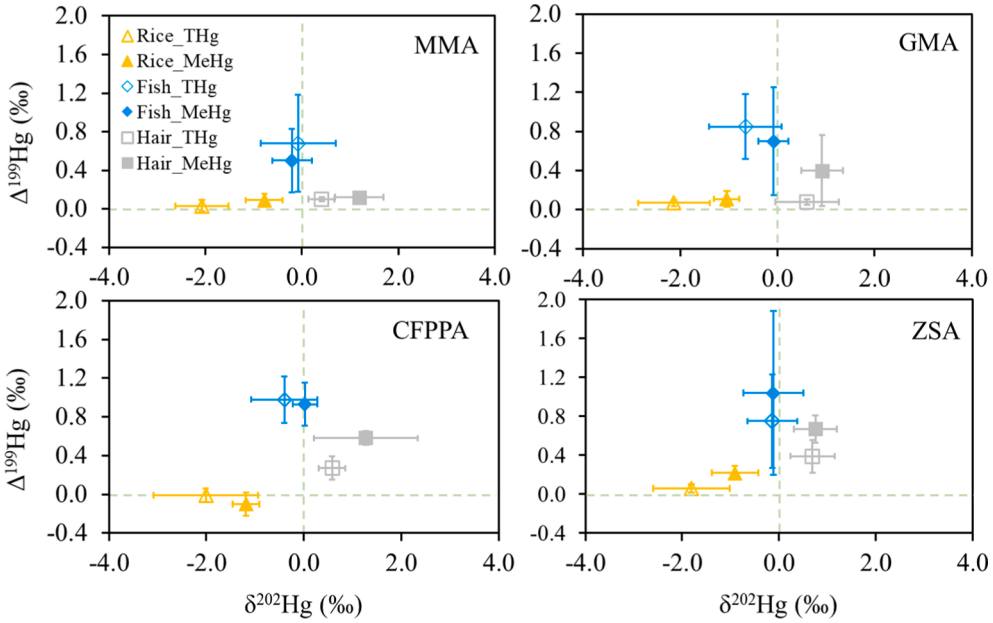

Fig. 2. δ^{202}Hg and Δ^{199}Hg values in THg and MeHg of rice, fish and hair samples in four study areas.

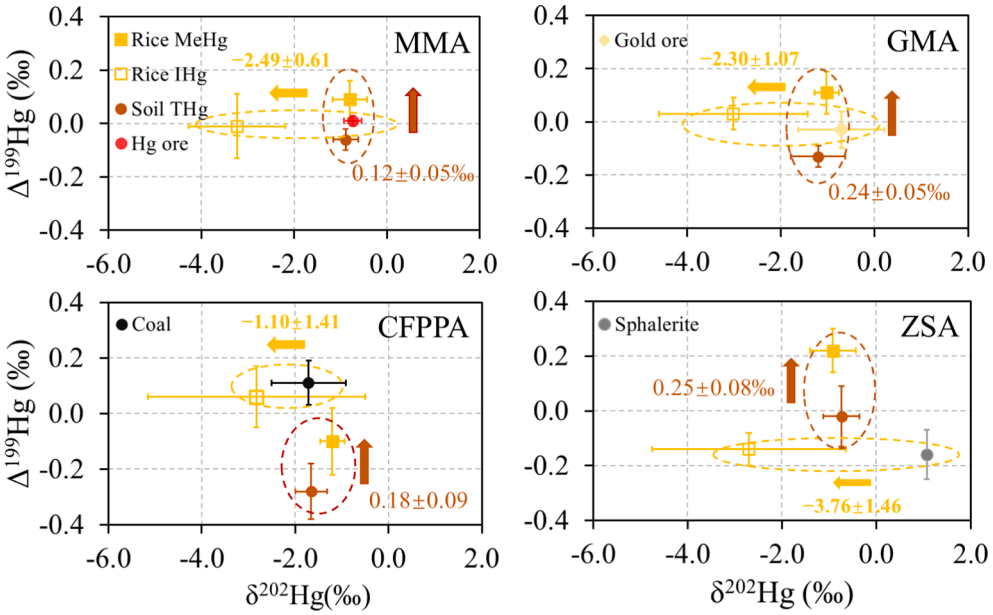

Fig. 3. δ^{202}Hg and Δ^{199}Hg values in rice MeHg and IHg in four study areas.

indicating fish MeHg potentially originated from plankton.

As stated above, IHg was a unneglected part of THg in fish muscle with a range ratio of 31 % to 79 %. The variability of $\delta^{202}Hg_{IHg}$ (−4.56 ‰ to 1.20 ‰) was larger than that of $\delta^{202}Hg_{MeHg}$ (−0.8 ‰ to 0.7 ‰), and the $\Delta^{199}Hg_{IHg}$ in fish samples showed significantly positive values with an average of 0.83 ± 0.43 ‰ (Table S5). However, the $\Delta^{199}Hg_{IHg}$ showed totally different values with those in water and sediment, which were close to 0 (Feng et al., 2010; Li et al., 2019; Liu et al., 2012). The$\Delta^{199}Hg_{IHg}$ values in plankton samples averaged at 0.45 ± 0.25 ‰ (Masbou et al., 2013). Due to no significant MIF of Hg during trophic transfer and metabolic processes (Laffont et al., 2021), the significantly positive $\Delta^{199}Hg_{IHg}$ values in fish muscles potentially originated from plankton or demethylation of MeHg in fish body. As shown in Fig. S2, the slope of $\Delta^{199}Hg_{IHg}/\Delta^{201}Hg_{IHg}$ was 1.08 ± 0.11, which was located between 1.21 ± 0.06 ($\Delta^{199}Hg_{MeHg}/\Delta^{201}Hg_{MeHg}$) and 1.00 ($\Delta^{199}$Hg/$\Delta^{201}$Hg) induced by photoreduction of Hg(II)), suggesting that IHg in fish muscle partially derived from *in vivo* demethylation of MeHg. No significant difference was observed between $\Delta^{199}Hg_{IHg}$ (0.83 ± 0.43 ‰) and $\Delta^{199}Hg_{MeHg}$ (0.80 ± 0.55 ‰) in fish samples (Fig. S1), which also indicated that demethylation of MeHg was an important source of IHg in fish body.

3.3. Human MeHg exposure pathways

The mean concentrations of THg and MeHg in hair samples were significantly higher ($p < 0.05$) in MMA than the other three areas (Table 1). Hair THg concentrations averaged at 2080 ± 1160 ng/g in MMA, which exceeded the international limit for hair THg (1000 ng/g) recommended by the United States Environmental Protection Agency (USEPA, 1997). Therefore, the local population, especially for those

(women and children) are sensitive to Hg, in MMA are at potential risks of Hg exposure. The THg concentrations in diet in MMA were highest among the four areas, and the dietary intake rates were similar, causing higher THg concentrations in hair in MMA (Wang et al., 2021). However, hair MeHg/THg ratio averaged at 44 ± 9 % in MMA, which was slightly lower than that in GMA (55 ± 11 %), but significantly lower ($p < 0.05$) than those in CFPPA (65 ± 11 %) and ZSA (71 ± 7 %). Human MeHg exposure pathways were calculated based on MeHg isotope data and discussed in detail below.

Human hair in the four study areas showed positive $\delta^{202}Hg_{MeHg}$ and $\Delta^{199}Hg_{MeHg}$ values (Fig. 2, Table S4). The $\Delta^{199}Hg_{MeHg}$ values in hair averaged at 0.12 ± 0.04 ‰ in MMA, 0.40 ± 0.36 ‰ in GMA, 0.58 ± 0.23 ‰ in CFPPA and 0.67 ± 0.14 ‰ in ZSA, and these values were within the range of fish and rice in the four study areas (Fig. 2). Therefore, the binary mixing isotope model described in Section 2.4 was used for quantifying the relative contributions of rice and fish consumption to human MeHg exposure. The $\Delta^{199}Hg_{MeHg}$ values rather than $\Delta^{199}Hg_{THg}$ in rice, fish and hair samples were directly used as model input, which shielded the disturbance of IHg. Model results revealed that the rice consumption contributed 84 ± 14 % to human MeHg exposure in MMA, 58 ± 26 % in GMA, 34 ± 15 % in CFPPA and 52 ± 20 % in ZSA on average. This indicated that rice consumption dominated human MeHg exposure in MMA, and the rice and fish consumption contributed nearly equally in GMA and ZSA (Fig. 4). The rice MeHg concentrations showed highest levels in MMA among the four study areas, and fish consumption was minimal for local residents (3.3 g/d) (NBS, 2021), resulting in high MeHg exposure from rice consumption in MMA.

However, these percentage contribution numbers were much lower than those estimated using a traditional dietary model, which estimated that the contribution of rice consumption to human MeHg exposure was 94 %±4% in MMA, 97 %±3% in GMA, 94 %±3% in CFPPA and 88 % ±8% in ZSA on average (Fig. 4) (Wang et al., 2021). The dietary model ignored individual differences on daily rice intake, and the data obtained from the questionnaire may cause large uncertainties in the estimation. As well, the bio-accessibilities of MeHg in rice and fish were not considered in the dietary model, and the simulation experiment found that the bio-accessibility of rice and fish MeHg averaged at 41 ± 9 % and 61 ± 14 %, respectively (Gong et al., 2018), indicating that traditional dietary model overestimated human MeHg exposure from rice consumption. In contrast, the binary mixing model based on MIF data can directly evaluate human MeHg exposure sources without these interfering factors. Additionally, the contribution ratios calculated by $\Delta^{199}Hg_{MeHg}$ values were much different from the results (Table S6) deduced by $\Delta^{199}Hg_{THg}$, illustrating IHg induced uncertainties when using THg isotopes to identify MeHg exposure pathways.

$\delta^{202}Hg_{MeHg}$ values in hair samples averaged at 1.19 ± 0.50 ‰ in MMA, 0.92 ± 0.43 ‰ in GMA, 1.27 ± 0.41 ‰ in CFPPA and 0.75 ± 0.44 ‰ in ZSA, showing positive shifts from those in rice and fish in the four areas. The shifts of $\delta^{202}Hg_{MeHg}$ from rice/fish to hair were calculated using the formula described in Section 2.5. Results from the calculation showed shifts of 1.88 ± 0.37 ‰, 1.54 ± 0.45 ‰, 1.61 ± 0.28 ‰ and 1.38 ± 0.37 ‰ in $\delta^{202}Hg_{MeHg}$ from diet (fish and rice) to hair in MMA, GMA, CFPPA and ZSA, respectively (Fig. 5). After being consumed by human, MeHg in the diet would be partially demethylated in the intestinal tract, resulting in lighter isotopes in feces or urine and enrichment of heavier isotopes in human hair (Du et al., 2020; Sherman et al., 2013). The shifts of $\delta^{202}Hg_{MeHg}$ in this study were close to the values of 1.7–2.2 ‰ in $\delta^{202}Hg_{THg}$ from fish to hair of fish consumers, but were much lower than the values of 2.5–2.7 ‰ in $\delta^{202}Hg_{THg}$ from rice to hair of rice consumers (Bonsignore et al., 2015; Du et al., 2018; Laffont et al., 2009; Laffont et al., 2011; Li et al., 2014; Sherman et al., 2013). In Europe and North America, MeHg was the dominant form (>90 %) of Hg in fish and human hair (Beckers et al., 2017), therefore the shifts were comparable. By contrast, the MeHg/THg ratios in the rice samples showed large ranges (9 % to 76 %, median: 49.5 %), and those in the paired human hair samples ranged from 25 % to 96 % (median: 58 %) (Du et al., 2018). Therefore, shifts of $\delta^{202}Hg_{THg}$ from diet to human hair were significantly impacted by IHg input by non-fish consumption. The MeHg isotopes rather than THg isotopes should be used for assessing the sources of human MeHg exposure to eliminate the interference from IHg.

4. Conclusions

Results from this study provide new insights for tracing Hg pollution and human MeHg exposure sources. We innovatively discovered that the rice IHg showed comparable $\Delta^{199}Hg$ values with those of raw ore materials and coal, and slightly positive shifts of $\Delta^{199}Hg$ (~0.2 ‰) occurred from soil IHg to rice MeHg, suggesting that MeHg and IHg isotopes in rice grain can be used to trace IHg and MeHg pollution sources. Simultaneously, the sources of MeHg and IHg in fish were identified by specific Hg isotopes. It was observed that MeHg was originated from plankton and IHg was partially from demethylation of MeHg in fish body. This study firstly measured the specific Hg isotopes to identify human MeHg exposure in typical Hg-emission areas. The binary mixing model identified human MeHg exposure pathways can overcome large uncertainties of daily intake and bio-accessibility and ignore the interference of IHg. The MDF of MeHg from fish/rice to hair samples can also be used to trace human metabolic processes and human MeHg exposure sources.

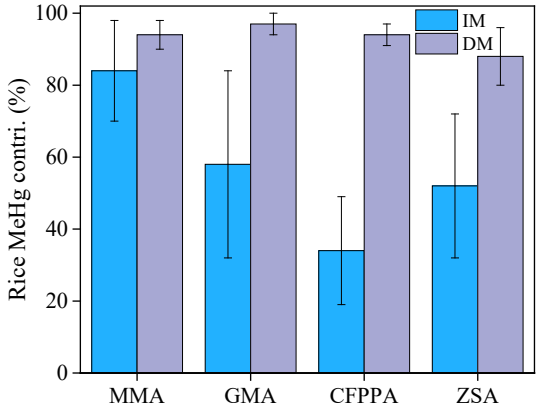

Fig. 4. Relative contribution of rice consumption on human MeHg exposure by isotope model (IM) and dietary model (DM) in four study areas.

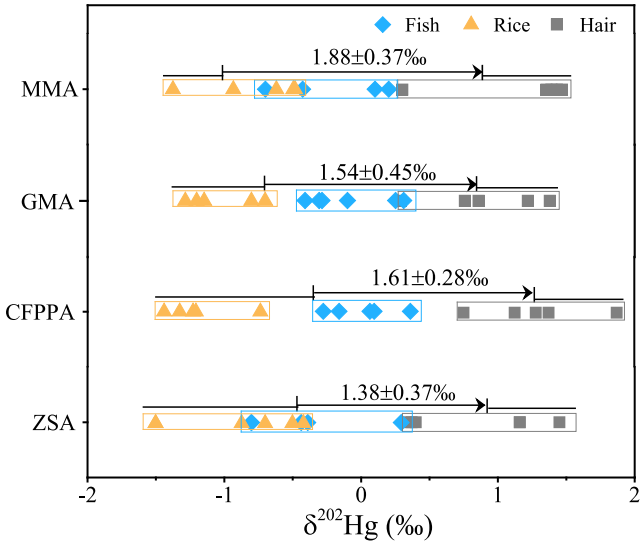

Fig. 5. The shifts of $\delta^{202}Hg_{MeHg}$ from diet (fish and rice) to hair in four study areas.

This study implicates that the MeHg CSIA method is an efficient approach for tracking human MeHg exposure and for making effective Hg pollution control strategies to reduce the health risks. To identify human Hg transformation processes, it is important for protecting human from the hazard of Hg. However, the specific metabolic processes in human body are still not fully understood. The MeHg-CSIA method can be adopted to track MeHg transform processes in human body in further study.

CRediT authorship contribution statement

Bo Wang: Data curation, Formal analysis, Methodology, Visualization, Writing – original draft, Writing – review & editing. **Shaochen Yang:** Conceptualization, Methodology, Writing – review & editing. **Ping Li:** Conceptualization, Formal analysis, Resources, Funding acquisition, Project administration, Writing – review & editing. **Chongyang Qin:** Conceptualization, Writing – review & editing. **Chuan Wang:** Conceptualization, Methodology. **Muhammad Ubaid Ali:** Data curation, Writing – review & editing. **Runsheng Yin:** Data curation, Writing – review & editing. **Laurence Maurice:** Data curation, Writing – review & editing. **David Point:** Data curation, Writing – review & editing. **Jeroen E. Sonke:** Data curation, Writing – review & editing. **Leiming Zhang:** Data curation, Formal analysis, Writing – review & editing. **Xinbin Feng:** Formal analysis, Resources, Funding acquisition, Project administration, Writing – review & editing.

Declaration of Competing Interest

The authors declare that they have no known competing financial interests or personal relationships that could have appeared to influence the work reported in this paper.

Data availability

Data will be made available on request.

Acknowledgments

This study was funded by the National Natural Science Foundation of China (U1812403, 41921004, 41622208), the CAS Interdisciplinary Innovation Team (JCTD-2020-20), and CAS Youth Innovation Promotion Association (Y2021106).

Appendix A. Supplementary material

Supplementary data to this article can be found online at https://doi.org/10.1016/j.envint.2023.107891.

References

Beckers, F., Rinklebe, J., 2017. Cycling of mercury in the environment: Sources, fate, and human health implications: a review. Crit. Rev. Environ. Sci. Technol. 47 (9), 693–794.
Bergquist, B.A., Blum, J.D., 2007. Mass-dependent and -independent fractionation of Hg isotopes by photoreduction in aquatic systems. Science. 318 (5849), 417–420.
Blum, J.D., Bergquist, B.A., 2007. Reporting of variations in the natural isotopic composition of mercury. Anal. Bioanal. Chem. 388 (2), 353–359.
Blum, J.D., Sherman, L.S., Johnson, M.W., 2014. Mercury Isotopes in Earth and Environmental Sciences. Annu. Rev. Earth Pl. Sc. 42 (1), 249–269.
Bonsignore, M., Tamburrino, S., Oliveri, E., Marchetti, A., Durante, C., Berni, A., Quinci, E., Sprovieri, M., 2015. Tracing mercury pathways in Augusta Bay (southern Italy) by total concentration and isotope determination. Environ. Pollut. 205, 178–185.
Chen, L., Liang, S., Liu, M., Yi, Y., Mi, Z., Zhang, Y., Li, Y., Qi, J., Meng, J., Tang, X., Zhang, H., Tong, Y., Zhang, W., Wang, X., Shu, J., Yang, Z., 2019. Trans-provincial health impacts of atmospheric mercury emissions in China. Nat, Commun, p. 10.
Cheng, J.P., Gao, L.L., Zhao, W.C., Liu, X.J., Sakamoto, M., Wang, W.H., 2009. Mercury levels in fisherman and their household members in Zhoushan, China: impact of public health. Sci. Total Environ. 407 (8), 2625–2630.
Clarkson, T.W., Magos, L., 2006. The toxicology of mercury and its chemical compounds. Crit. Rev. Toxicol. 36 (8), 609–662.
Demers, J.D., Blum, J.D., Zak, D.R., 2013. Mercury isotopes in a forested ecosystem: Implications for air-surface exchange dynamics and the global mercury cycle. Global Biogeochem. Cy. 27 (1), 222–238.
Driscoll, C.T., Mason, R.P., Chan, H.M., Jacob, D.J., Pirrone, N., 2013. Mercury as a global pollutant: sources, pathways, and effects. Environ. Sci. Technol. 47 (10), 4967–4983.
Du, B., Feng, X., Li, P., Yin, R., Yu, B., Sonke, J.E., Guinot, B., Anderson, C.W.N., Maurice, L., 2018. Use of mercury isotopes to quantify mercury exposure sources in inland populations. China. Environ. Sci. Technol. 52 (9), 5407–5416.
Du, B.; Yin, R.; Fu, X.; Li, P.; Feng, X.; Maurice, L. 2020; Use of mercury isotopes to quantify sources of human inorganic mercury exposure and metabolic processes in the human body. Environ. Int. 147:106336-106336.
Epov, V.N., Rodriguez-Gonzalez, P., Sonke, J.E., Tessier, E., Amouroux, D., Maurice Bourgoin, L., Donard, O.F.X., 2008. Simultaneous determination of species-specific isotopic composition of Hg by gas chromatography coupled to multicollector ICPMS. Anal. Chem. 80 (10), 3530–3538.
Estrade, N., Carignan, J., Sonke, J.E., Donard, O.F.X., 2010. Measuring Hg isotopes in bio-geo-environmental reference materials. Geostand. Geoanal. Res. 34 (1), 79–93.
Feng, X., Foucher, D., Hintelmann, H., Yan, H., He, T., Qiu, G., 2010. Tracing mercury contamination sources in sediments using mercury isotope compositions. Environ. Sci. Technol. 44 (9), 3363–3368.
Feng, X., Li, P., Qiu, G., Wang, S., Li, G., Shang, L., Meng, B., Jiang, H., Bai, W., Li, Z., Fu, X., 2008. Human exposure to methylmercury through rice intake in mercury mining areas, guizhou province, china. Environ. Sci. Technol. 42 (1), 326–332.
GB2762. 2017; Maximum levels of contaminants in foods. The National Standard of the People's Republic of China.
Gong, Y., Nunes, L.M., Greenfield, B., Qin, Z., Yang, Q.Q., Huang, L., Bu, W.B., Zhong, H., 2018. Bioaccessibility-corrected risk assessment of urban dietary methylmercury exposure via fish and rice consumption in China. Sci. Total Environ. 630, 222–230.
Hintelmann, H., Nguyen, H., 2005. Extraction of methylmercury from tissue and plant samples by acid leaching. Anal. Bioanal. Chem. 381 (2), 360–365.
Janssen, S.E., Johnson, M.W., Blum, J.D., Barkay, T., Reinfelder, J.R., 2015. Separation of monomethylmercury from estuarine sediments for mercury isotope analysis. Chem. Geol. 411, 19–25.
Kritee, K., Motta, L.C., Blum, J.D., Tsui, M.-T.-K., Reinfelder, J.R., 2018. Photomicrobial visible light-induced magnetic mass independent fractionation of mercury in a marine microalga. Acs Earth and Space Chemistry. 2 (5), 432–440.
Kwon, S.Y., Blum, J.D., Carvan, M.J., Basu, N., Head, J.A., Madenjian, C.P., David, S.R., 2012. Absence of fractionation of mercury isotopes during trophic transfer of methylmercury to freshwater fish in captivity. Environ. Sci. Technol. 46 (14), 7527–7534.
Kwon, S.Y., Blum, J.D., Chen, C.Y., Meattey, D.E., Mason, R.P., 2014. Mercury isotope study of sources and exposure pathways of methylmercury in estuarine food webs in the northeastern US. Environ. Sci. Technol. 48 (17), 10089–10097.
Kwon, S.Y., Blum, J.D., Yin, R., Tsui, M.-T.-K., Yang, Y.H., Choi, J.W., 2020. Mercury stable isotopes for monitoring the effectiveness of the Minamata Convention on Mercury. Earth-Sci, Rev, p. 203.
Laffont, L., Menges, J., Goix, S., Gentes, S., Maury-Brachet, R., Sonke, J.E., Legeay, A., Gonzalez, P., Rinaldo, R., Maurice, L., 2021. Hg concentrations and stable isotope variations in tropical fish species of a gold-mining-impacted watershed in French Guiana. Environ. Sci. Pollut. R. 28 (43), 60609–60621.
Laffont, L., Sonke, J.E., Maurice, L., Hintelmann, H., Pouilly, M., Bacarreza, Y.S., Perez, T., Behra, P., 2009. Anomalous mercury isotopic compositions of fish and human hair in the bolivian amazon. Environ. Sci. Technol. 43 (23), 8985–8990.
Laffont, L., Sonke, J.E., Maurice, L., Monrroy, S.L., Chincheros, J., Amouroux, D., Behra, P., 2011. Hg speciation and stable isotope signatures in human hair as a tracer for dietary and occupational exposure to mercury. Environ Sci Technol. 45 (23), 9910–9916.
Li, K., Lin, C.-J., Yuan, W., Sun, G., Fu, X., Feng, X., 2019. An improved method for recovering and preconcentrating mercury in natural water samples for stable isotope analysis. J. Anal. Atom. Spectrom. 34 (11), 2303–2313.
Li, M., Schartup, A.T., Valberg, A.P., Ewald, J.D., Krabbenhoft, D.P., Yin, R., Bolcom, P. H., Sunderland, E.M., 2016. Environmental Origins of Methylmercury Accumulated in Subarctic Estuarine Fish Indicated by Mercury Stable Isotopes. Environ. Sci. Technol. 50 (21), 11559–11568.
Li, M., Sherman, L.S., Blum, J.D., Grandjean, P., Mikkelsen, B., Weihe, P., Sunderland, E. M., Shine, J.P., 2014. Assessing sources of human methylmercury exposure using stable mercury isotopes. Environ. Sci. Technol. 48 (15), 8800–8806.
Li, P., Du, B.Y., Maurice, L., Laffont, L., Lagane, C., Point, D., Sonke, J.E., Yin, R.S., Lin, C. J., Feng, X.B., 2017. Mercury isotope signatures of methylmercury in rice samples from the wanshan mercury mining area, china: environmental implications. Environ. Sci. Technol. 51 (21), 12321–12328.
Li, P., Feng, X., Yuan, X., Chan, H.M., Qiu, G., Sun, G.-X., Zhu, Y.-G., 2012. Rice consumption contributes to low level methylmercury exposure in southern China. Environ. Int. 49, 18–23.
Liang, L., Horvat, M., Cernichiari, E., Gelein, B., Balogh, S., 1996. Simple solvent extraction technique for elimination of matrix interferences in the determination of methylmercury in environmental and biological samples by ethylation gas chromatography cold vapor atomic fluorescence spectrometry. Talanta. 43 (11), 1883–1888.
Liu, B., Yan, H., Wang, C., Li, Q., Guedron, S., Spangenberg, J.E., Feng, X., Dominik, J., 2012. Insights into low fish mercury bioaccumulation in a mercury-contaminated reservoir, Guizhou. China. Environ. Pollut. 160, 109–117.
Liu, J., Xu, X., Yu, S., Cheng, H., Hong, Y., Feng, X., 2014. Mercury pollution in fish from South China Sea: levels, species-specific accumulation, and possible sources. Environ. Res. 131, 160–164.

Liu, K., Wu, Q., Wang, L., Wang, S., Liu, T., Ding, D., Tang, Y., Li, G., Tian, H., Duan, L., Wang, X., Fu, X., Feng, X., Hao, J., 2019. Measure-specific effectiveness of air pollution control on china's atmospheric mercury concentration and deposition during 2013–2017. Environ. Sci. Technol. 53 (15), 8938–8946.
Liu, M., Chen, L., He, Y., Baumann, Z., Mason, R.P., Shen, H., Yu, C., Zhang, W., Zhang, Q., Wang, X., 2018. Impacts of farmed fish consumption and food trade on methylmercury exposure in China. Environ. Int. 120, 333–344.
Liu, Y.-F., Qi, H.-W., Bi, X.-W., Hu, R.-Z., Qi, L.-K., Yin, R.-S., Tang, Y.-Y., 2021. Mercury and sulfur isotopic composition of sulfides from sediment-hosted lead-zinc deposits in Lanping basin, Southwestern China. Chemical Geol. 559, 119910.
Masbou, J., Point, D., Sonke, J.E., 2013. Application of a selective extraction method for methylmercury compound specific stable isotope analysis (MeHg-CSIA) in biological materials. J. Anal. Atom. Spectrom. 28 (10).
Meng, M., Sun, R.Y., Liu, H.W., Yu, B., Yin, Y.G., Hu, L.G., Chen, J.B., Shi, J.B., Jiang, G. B., 2020. Mercury isotope variations within the marine food web of Chinese Bohai Sea: implications for mercury sources and biogeochemical cycling. J. Hazard. Mater. 384, 13.
Nbs, 2021. National Bureau of Statistics, Chinese Statistical Yearbook 2020. China Statistics Press, Beijing.
Perrot, V., Masbou, J., Pastukhov, M.V., Epov, V.N., Point, D., Berail, S., Becker, P.R., Sonke, J.E., Amouroux, D., 2016. Natural Hg isotopic composition of different Hg compounds in mammal tissues as a proxy for in vivo breakdown of toxic methylmercury. Metallomics. 8 (2), 170–178.
Qin, C., Chen, M., Yan, H., Shang, L., Yao, H., Li, P., Feng, X., 2018. Compound specific stable isotope determination of methylmercury in contaminated soil. Sci. Total Environ. 644, 406–412.
Qin, C., Du, B., Yin, R., Meng, B., Fu, X., Li, P., Zhang, L., Feng, X., 2020. Isotopic fractionation and source appointment of methylmercury and inorganic mercury in a paddy ecosystem. Environ. Sci. Technol. 54 (22), 14334–14342.
Qiu, G., Feng, X., Wang, S., Fu, X., Shang, L., 2009. Mercury distribution and speciation in water and fish from abandoned Hg mines in Wanshan, Guizhou province, China. Sci. Total Environ. 407 (18), 5162–5168.
Rosera, T.J., Janssen, S.E., Tate, M.T., Lepak, R.F., Ogorek, J.M., DeWild, J.F., Babiarz, C. L., Krabbenhoft, D.P., Hurley, J.P., 2020. Isolation of methylmercury using distillation and anion-exchange chromatography for isotopic analyses in natural matrices. Anal. Bioanal. Chem. 412 (3), 681–690.
Rothenberg, S.E., Yin, R.S., Hurley, J.P., Krabbenhoft, D.P., Ismawati, Y., Hong, C., Donohue, A., 2017. Stable mercury isotopes in polished rice (Oryza sativa L.) and hair from rice consumers. Environ. Sci. Technol. 51 (11), 6480–6488.
Selin, N.E., 2009. Global biogeochemical cycling of mercury: a review. Annu. Rev. Env. Resour. 34, 43–63.
Shao, D.D., Kang, Y., Cheng, Z., Wang, H.S., Huang, M.J., Wu, S.C., Chen, K.C., Wong, M. H., 2013. Hair mercury levels and food consumption in residents from the Pearl River Delta: South China. Food Chem. 136 (2), 682–688.
Sherman, L.S., Blum, J.D., Franzblau, A., Basu, N., 2013. New insight into biomarkers of human mercury exposure using naturally occurring mercury stable isotopes. Environ. Sci. Technol. 47 (7), 3403–3409.
Sun, R., Sonke, J.E., Heimbuerger, L.-E., Belkin, H.E., Liu, G., Shome, D., Cukrowska, E., Liousse, C., Pokrovsky, O.S., Streets, D.G., 2014. Mercury stable isotope signatures of world coal deposits and historical coal combustion emissions. Environ. Sci. Technol. 48 (13), 7660–7668.
Tsui, M.-T.-K., Blum, J.D., Kwon, S.Y., 2020. Review of stable mercury isotopes in ecology and biogeochemistry. Sci, Total Environ, p. 716.
Unep, 2019. Global Mercury assessment 2018. UNEP Chemicals and Health Branch, Geneva, Switzerland.
USEPA. 1997; Mercury Study Report to the Congress, Vol. IV: An assessment of exposure to mercury in the United States. USEPA: Washington, USA.
Usepa, 2002. Mercury in water by oxidation, purge and trap, and cold vapor atomic absorption fluorescence spectrometry. WA, USEPA.
Wang, B., Chen, M., Ding, L., Zhao, Y., Man, Y., Feng, L., Li, P., Zhang, L., Feng, X., 2021. Fish, rice, and human hair mercury concentrations and health risks in typical Hg-contaminated areas and fish-rich areas. China. Environ, Int, p. 154.
Wang, X., Wang, W.-X., 2019. The three 'B' of fish mercury in China: Bioaccumulation, biodynamics and biotransformation. Environ. Pollut. 250, 216–232.
Wu, Q., Wang, S., Li, G., Liang, S., Lin, C.-J., Wang, Y., Cai, S., Liu, K., Hao, J., 2016. Temporal trend and spatial distribution of speciated atmospheric mercury emissions in china during 1978–2014. Environ. Sci. Technol. 50 (24), 13428–13435.
Xu, Q., Zhao, L., Wang, Y., Xie, Q., Yin, D., Feng, X., Wang, D., 2018. Bioaccumulation characteristics of mercury in fish in the Three Gorges Reservoir. China. Environ. Pollut. 243, 115–126.
Xu, X.; Han, J.; Pang, J.; Wang, X.; Lin, Y.; Wang, Y.; Qiu, G. 2019; Methylmercury and inorganic mercury in Chinese commercial rice: Implications for overestimated human exposure and health risk. Environmental pollution (Barking, Essex : 1987). 258:113706-113706.
Yamakawa, A.; Takeuchi, A.; Shibata, Y.; Berail, S.; Donard, O.F.X. 2016; Determination of Hg isotopic compositions in certified reference material NIES No. 13 Human Hair by cold vapor generation multi-collector inductively coupled plasma mass spectrometry. Accredit. Qual. Assur. 21 (3):197-202.
Yang, S., Li, P., Liu, J., Ubaid Ali, M., Ding, L., Wang, B., 2022. Combining of C, N and specific Hg stable isotopes to track bioaccumulation of monomethylmercury in coastal and freshwater seafood. Food Chem., 134202
Yang, S., Wang, B., Qin, C., Yin, R., Li, P., Liu, J., Point, D., Maurice, L., Sonke, J.E., Zhang, L., Feng, X., 2021. Compound-Specific Stable Isotope Analysis Provides New Insights for Tracking Human Monomethylmercury Exposure Sources. Environ. Sci, Technol.
Yin, R., Deng, C., Lehmann, B., Sun, G., Lepak, R.F., Hurley, J.P., Zhao, C., Xu, G., Tan, Q., Xie, Z., Hu, R., 2019. Magmatic-hydrothermal origin of mercury in carlin-style and epithermal gold deposits in china: evidence from mercury stable isotopes. Acs Earth and Space Chem. 3 (8), 1631–1639.
Yin, R.; Feng, X.; Meng, B. 2013a; Stable Mercury Isotope Variation in Rice Plants (Oryza sativa L.) from the Wanshan Mercury Mining District, SW China. Environ. Sci. Technol. 47 (5):2238-2245.
Yin, R., Feng, X., Wang, J., Li, P., Liu, J., Zhang, Y., Chen, J., Zheng, L., Hu, T., 2013b. Mercury speciation and mercury isotope fractionation during ore roasting process and their implication to source identification of downstream sediment in the Wanshan mercury mining area, SW China. Chem. Geol. 336, 72–79.
Yuan, W., Sommar, J., Lin, C.-J., Wang, X., Li, K., Liu, Y., Zhang, H., Lu, Z., Wu, C., Feng, X., 2019. Stable isotope evidence shows re-emission of elemental mercury vapor occurring after reductive loss from foliage. Environ. Sci. Technol. 53 (2), 651–660.
Zhang, H., Feng, X., Larssen, T., Qiu, G., Vogt, R.D., 2010a. In Inland China, Rice, Rather than Fish, Is the Major Pathway for Methylmercury Exposure. Environ. Health Persp. 118 (9), 1183–1188.
Zhang, H.; Feng, X.; Larssen, T.; Shang, L.; Li, P. 2010b; Bioaccumulation of Methylmercury versus Inorganic Mercury in Rice (Oryza sativa L.) Grain. Environ. Sci. Technol. 44 (12):4499-4504.
Zhang, Y., Song, Z., Huang, S., Zhang, P., Peng, Y., Wu, P., Gu, J., Dutkiewicz, S., Zhang, H., Wu, S., Wang, F., Chen, L., Wang, S., Li, P., 2021. Global health effects of future atmospheric mercury emissions. Nat. Commun. 12 (1).
Zhao, H., Yan, H., Zhang, L., Sun, G., Li, P., Feng, X., 2019. Mercury contents in rice and potential health risks across China. Environ. Int. 126, 406–412.